



Carles Pelejero<sup>1,2</sup>, Ariadna Martínez-Dios<sup>1</sup>, César Nicolás Rodríguez-Díaz<sup>1</sup>, Antonio Cattaneo<sup>3</sup>, Juancho Movilla<sup>1,4</sup>, Jaume Dinarès-Turell<sup>5</sup> and Eva Calvo<sup>1</sup>

<sup>1</sup> Institut de Ciències del Mar, CSIC, Barcelona, Catalonia, Spain  
<sup>2</sup> Institució Catalana de Recerca i Estudis Avançats, Barcelona, Catalonia, Spain  
<sup>3</sup> Institut Français de Recherche pour l'Exploitation de la Mer, Plouzané, France  
<sup>4</sup> Estació d'Investigació Jaume Ferrer, COB, IEO, Menorca, Balearic Islands, Spain  
<sup>5</sup> Istituto Nazionale di Geofisica e Vulcanologia (INGV), Rome, Italy



## 1. Oceanographic setting and age models

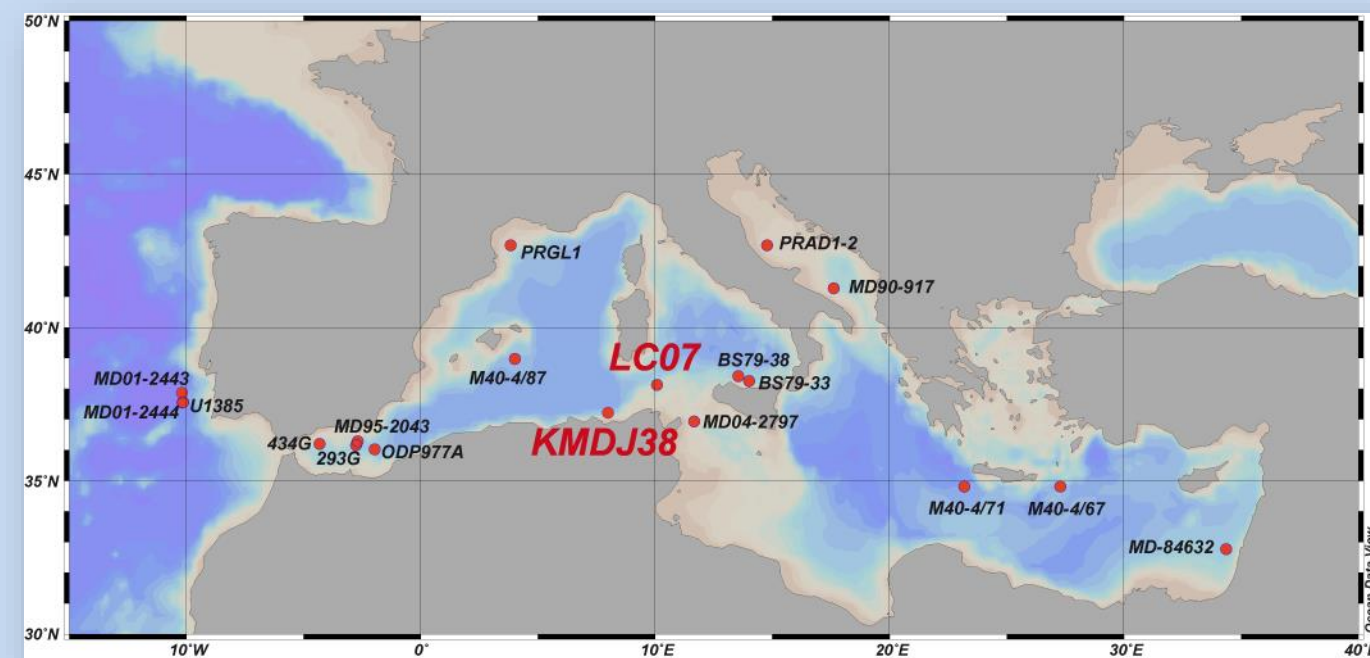


Figure 1. Bathymetric map of the Mediterranean Sea with the location of the studied cores (LC07 and KMDJ38) together with other cores for which, at least, one continuous G/I cycle based on molecular biomarkers, reaching modern times, has been published.

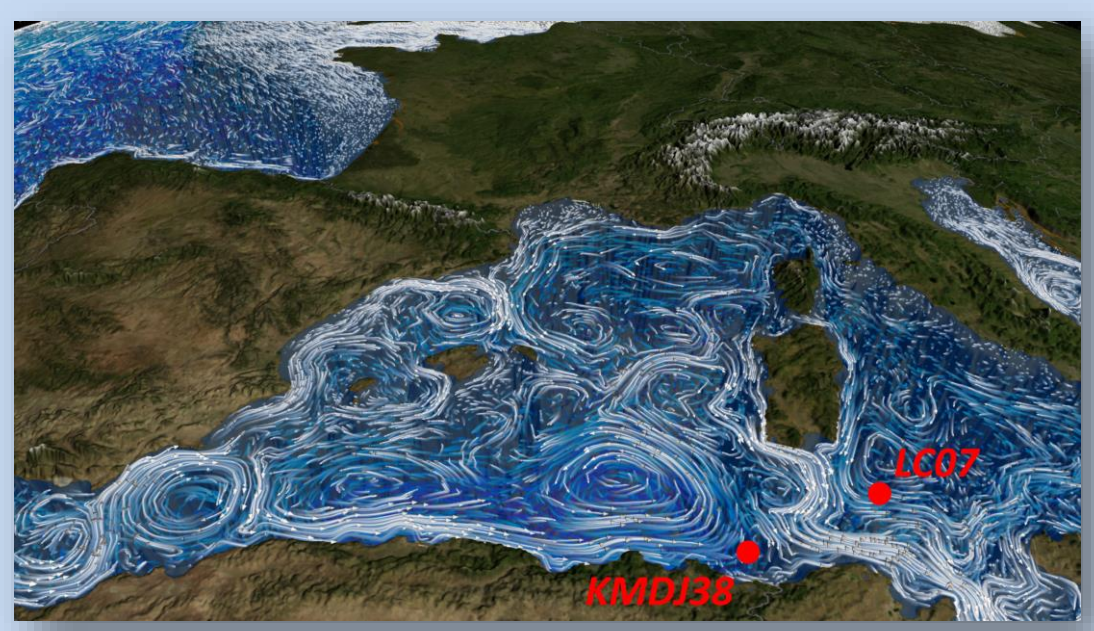
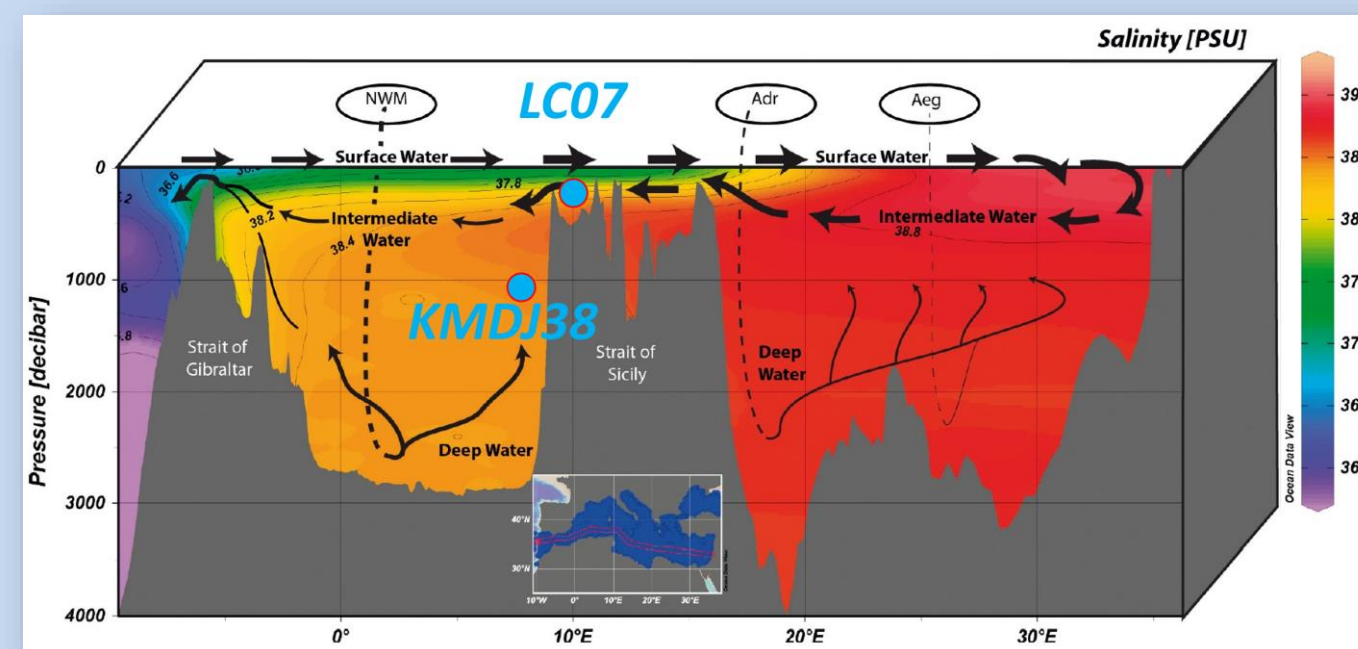


Figure 2. Simulation of surface (white) and deep (blue) current flows in the Mediterranean Sea during year 2005 using the ECCO2 high resolution ocean and sea ice model (obtained from <http://svs.gsfc.nasa.gov/3820>). The location of the studied cores (LC07 and KMDJ38) are indicated.

Figure 3. Cross section showing the distribution of salinity and the general circulation of the Mediterranean Sea. The thicknesses of the arrows indicate the relative flow rates. Major deep-water formation areas are identified. Adapted from Powley et al. 2018. The locations of the studied cores (LC07 and KMDJ38) are indicated.



LC07: 38°8.72'N, 10°4.73'E; 23.66 m, 488 m depth

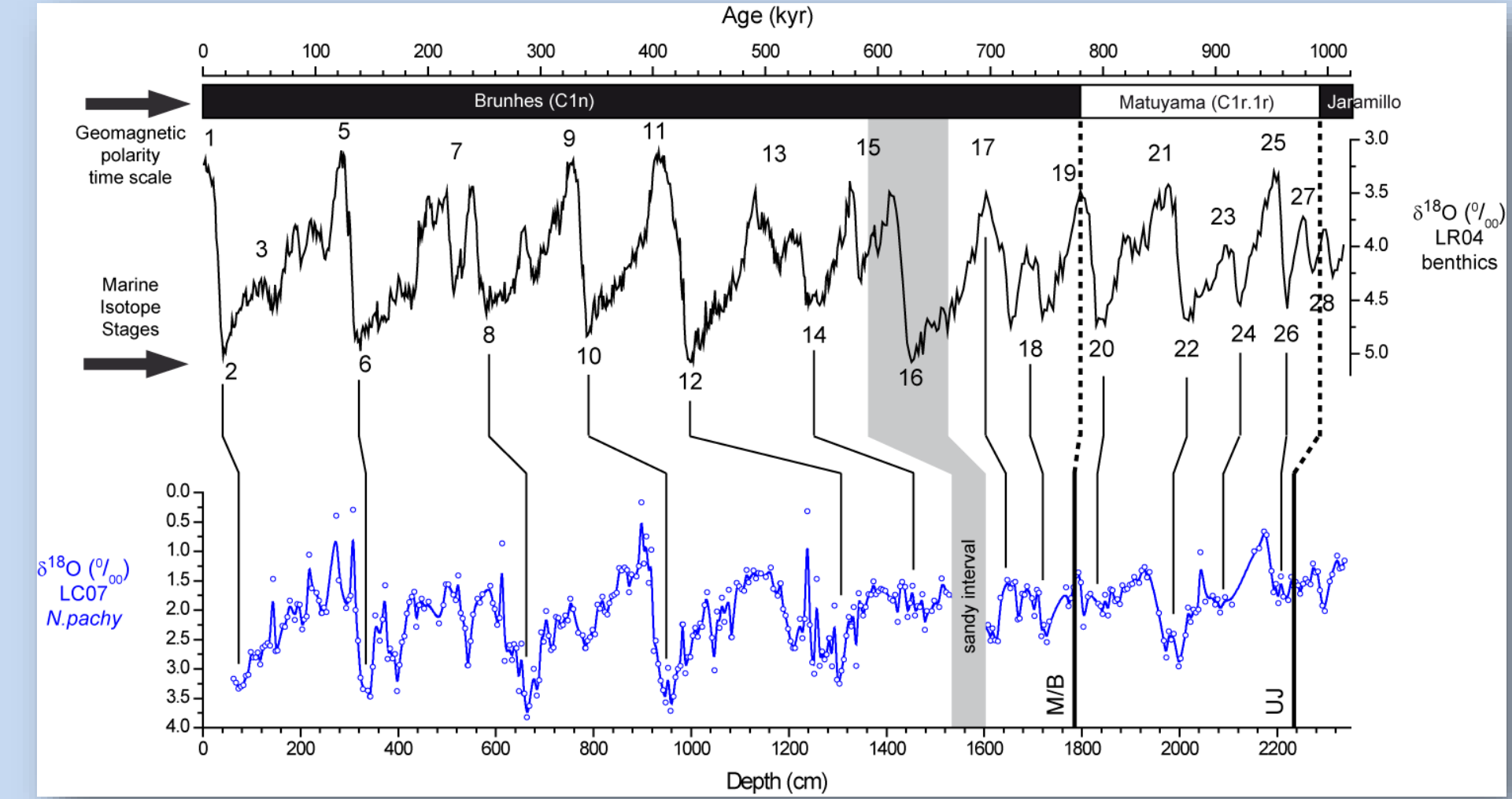


Figure 4. Age model of core LC07 based on the tuning of *Neoglobobulimina pachyderma* (dextral)  $\delta^{18}\text{O}$  (data from Dinarès-Turell et al. 2003) with the LR04 benthic  $\delta^{18}\text{O}$  stack (Lisiecki and Raymo 2005). The occurrence of a foraminifer-rich sandy interval and the position of the Matuyama/Brunhes (M/B) and upper Jaramillo (UJ) reversal boundaries (also used in the age model) are indicated.

KMDJ38: 37°13.49'N, 8°0.01'E; 8.07 m, 1057 m depth

Figure 5. Age model of core KMDJ38 based on four  $^{14}\text{C}$  measurements (black triangles, data from Giresse et al., 2013) and the LGM at 18 kyr.

## 2. Choices of $U^K_{37}$ -SST calibrations

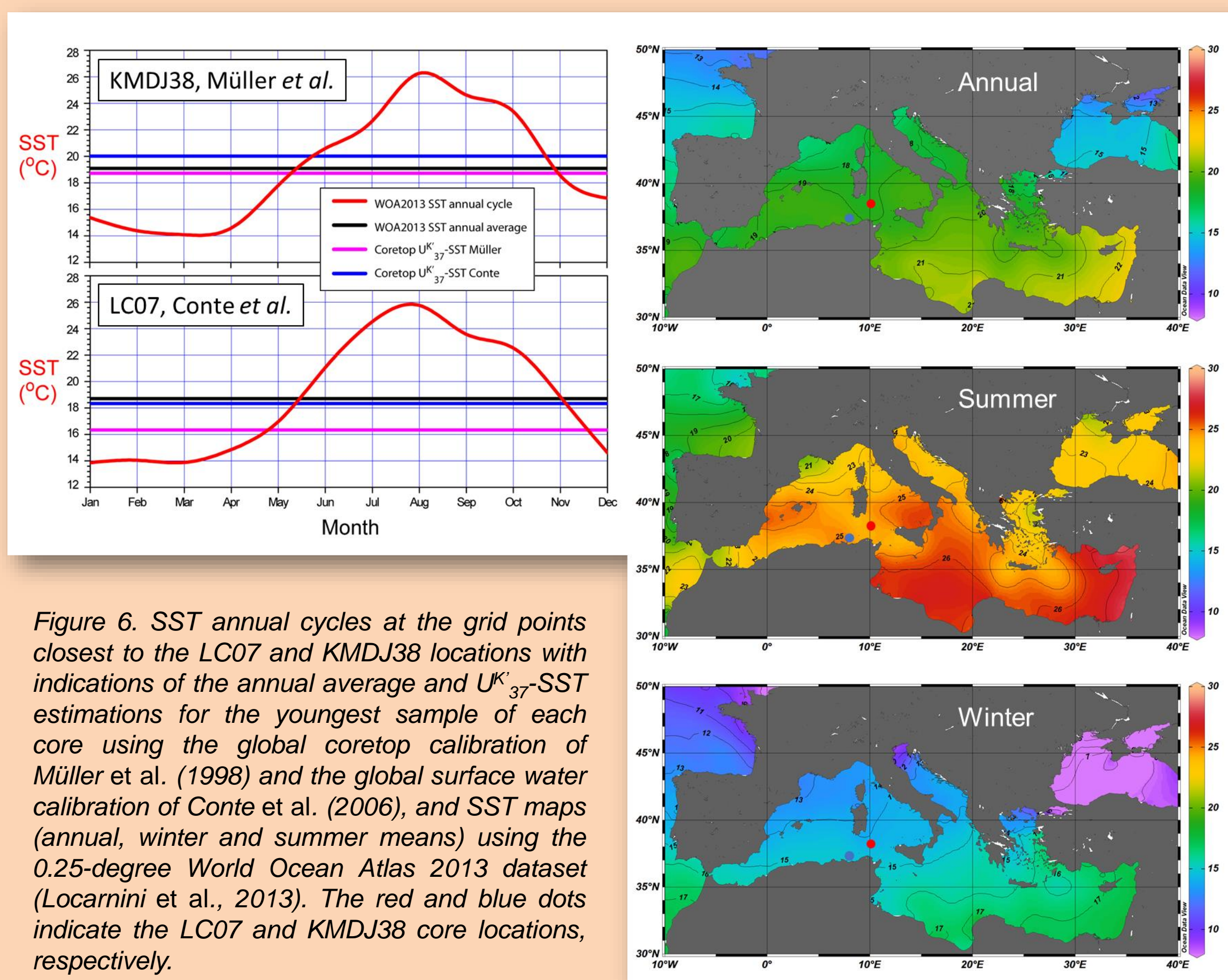


Figure 6. SST annual cycles at the grid points closest to the LC07 and KMDJ38 locations with indications of the annual average and  $U^K_{37}$ -SST estimations for the youngest sample of each core using the global coretop calibration of Müller et al. (1998) and the global surface water calibration of Conte et al. (2006), and SST maps (annual, winter and summer means) using the 0.25-degree World Ocean Atlas 2013 dataset (Locarnini et al., 2013). The red and blue dots indicate the LC07 and KMDJ38 core locations, respectively.

## 3. $U^K_{37}$ -SST paleoreconstructions

$U^K_{37}$ -SST vs  $\delta^{18}\text{O}$  Strait of Sicily

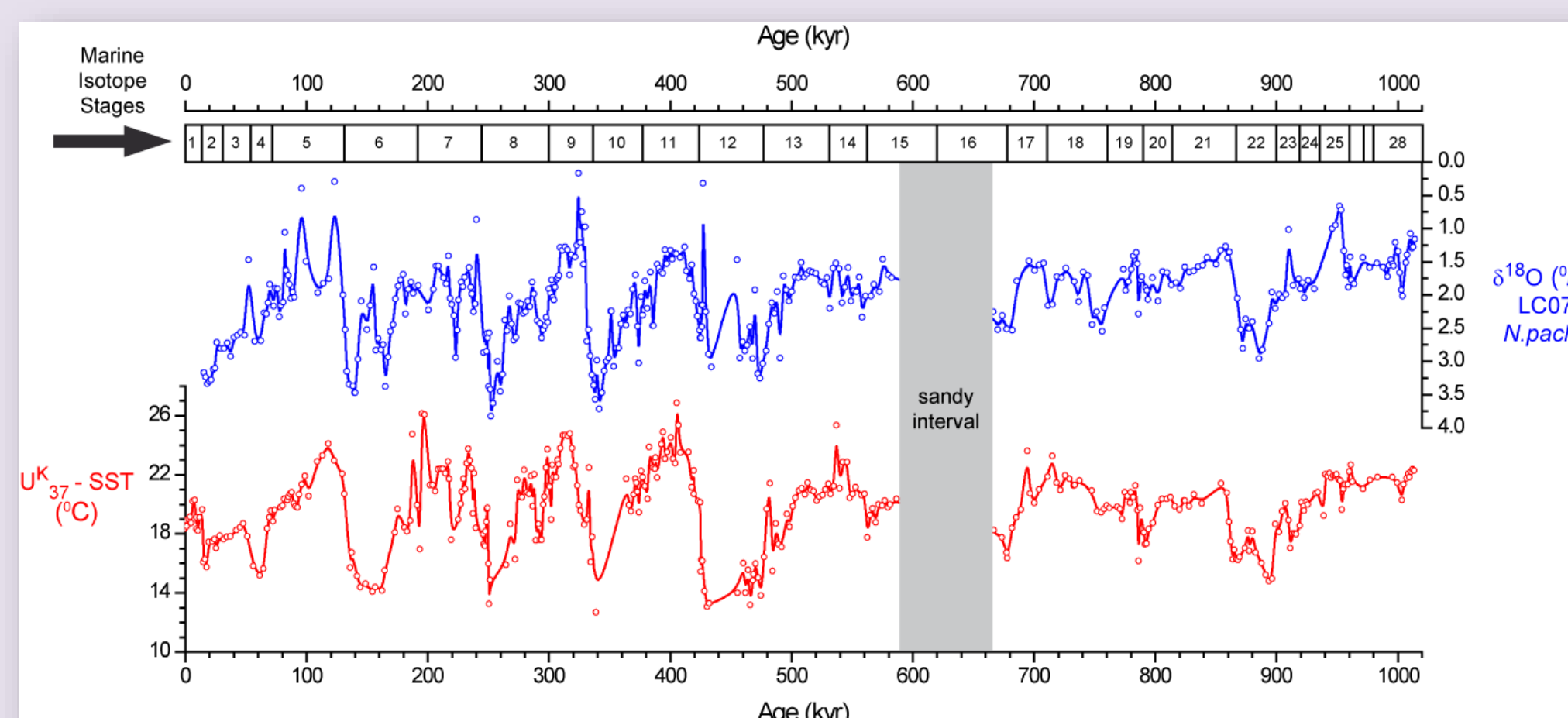


Figure 7. Records of *N. pachyderma* (dextral)  $\delta^{18}\text{O}$  (Dinarès-Turell et al. 2003) and  $U^K_{37}$ -SST (Martínez-Dios et al. 2021) for core LC07 for the last ~1 million years.

Algerian Margin

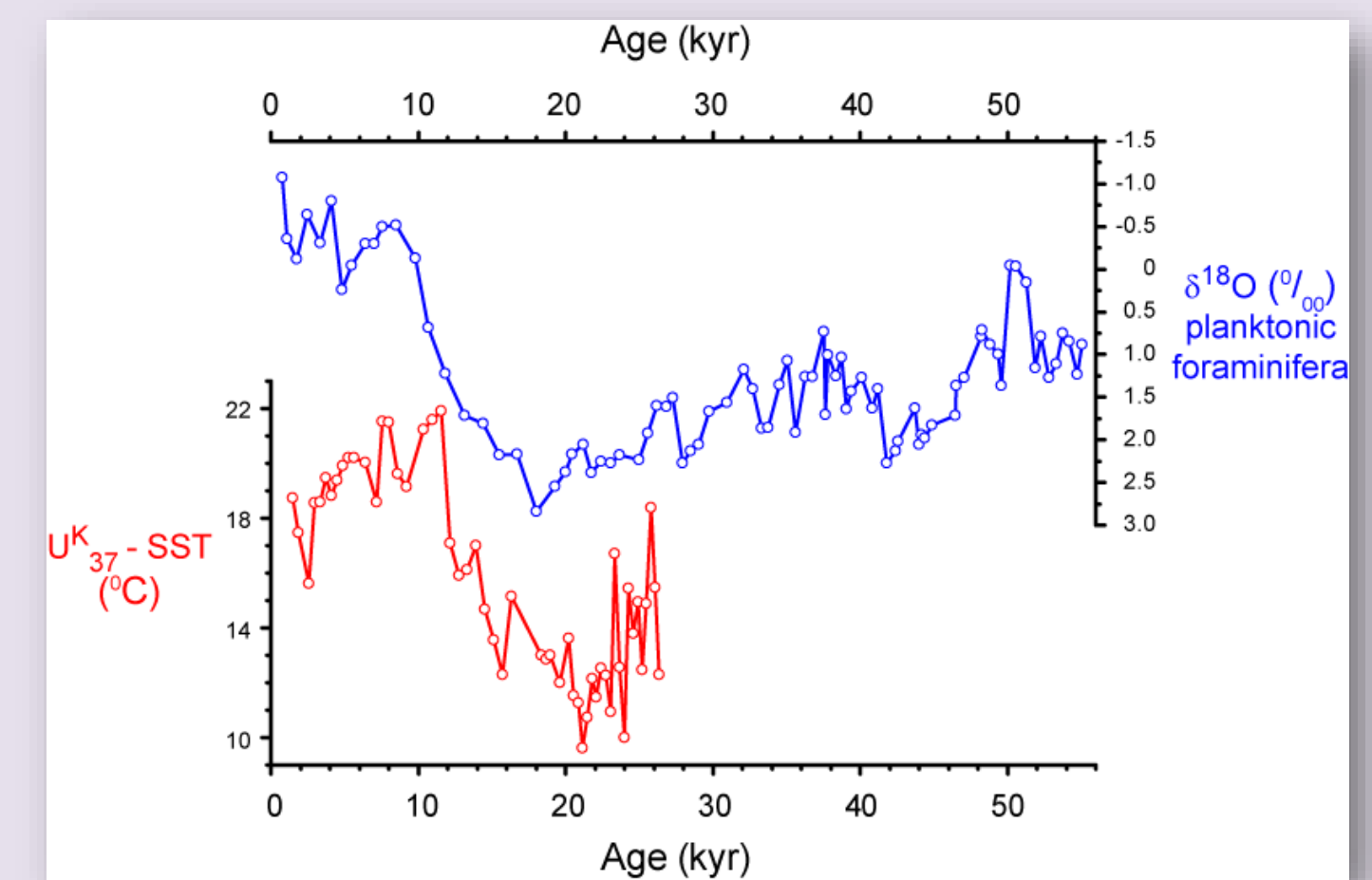


Figure 8. Records of planktonic foraminifera  $\delta^{18}\text{O}$  (Giresse et al., 2013) and  $U^K_{37}$ -SST (this study) for core KMDJ38 for the last 55 kyr.

### Comparisons with other records

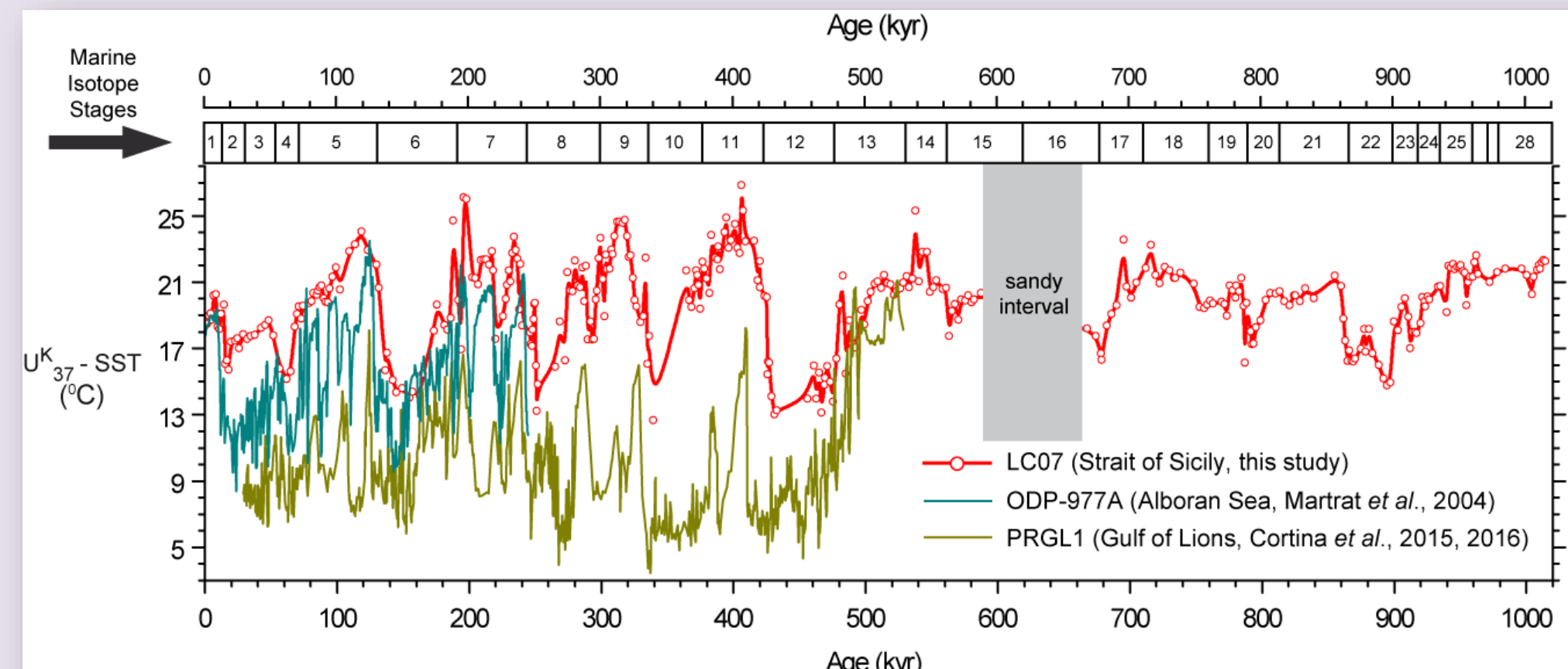


Figure 9. Comparison of the  $U^K_{37}$ -SST record from core LC07 (Martínez-Dios et al. 2021) with the two longest  $U^K_{37}$ -SST records published so far in the Mediterranean Sea (data for ODP-977A in the Alboran Sea is from Martrat et al. 2004 and these for PRGL1, in the Gulf of Lions, are from Cortina et al. 2015, 2016).

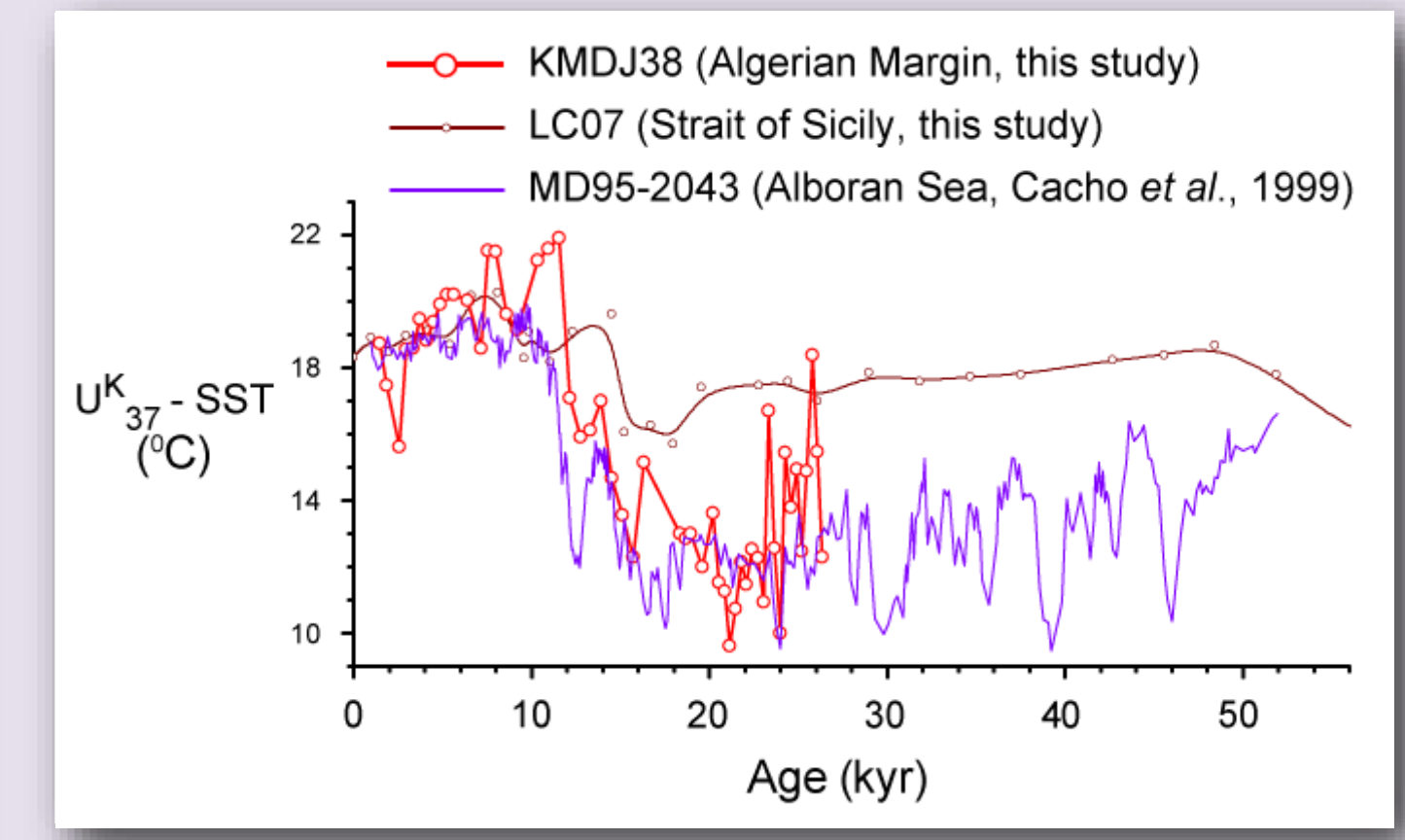


Figure 10. Comparison of the  $U^K_{37}$ -SST records from cores KMDJ38 (Algerian Margin, this study), LC07 (Strait of Sicily, Martínez-Dios et al. 2021) and MD95-2043 (Alboran Sea, Cacho et al. 1999).

## 4. Phytoplankton dynamics

Strait of Sicily

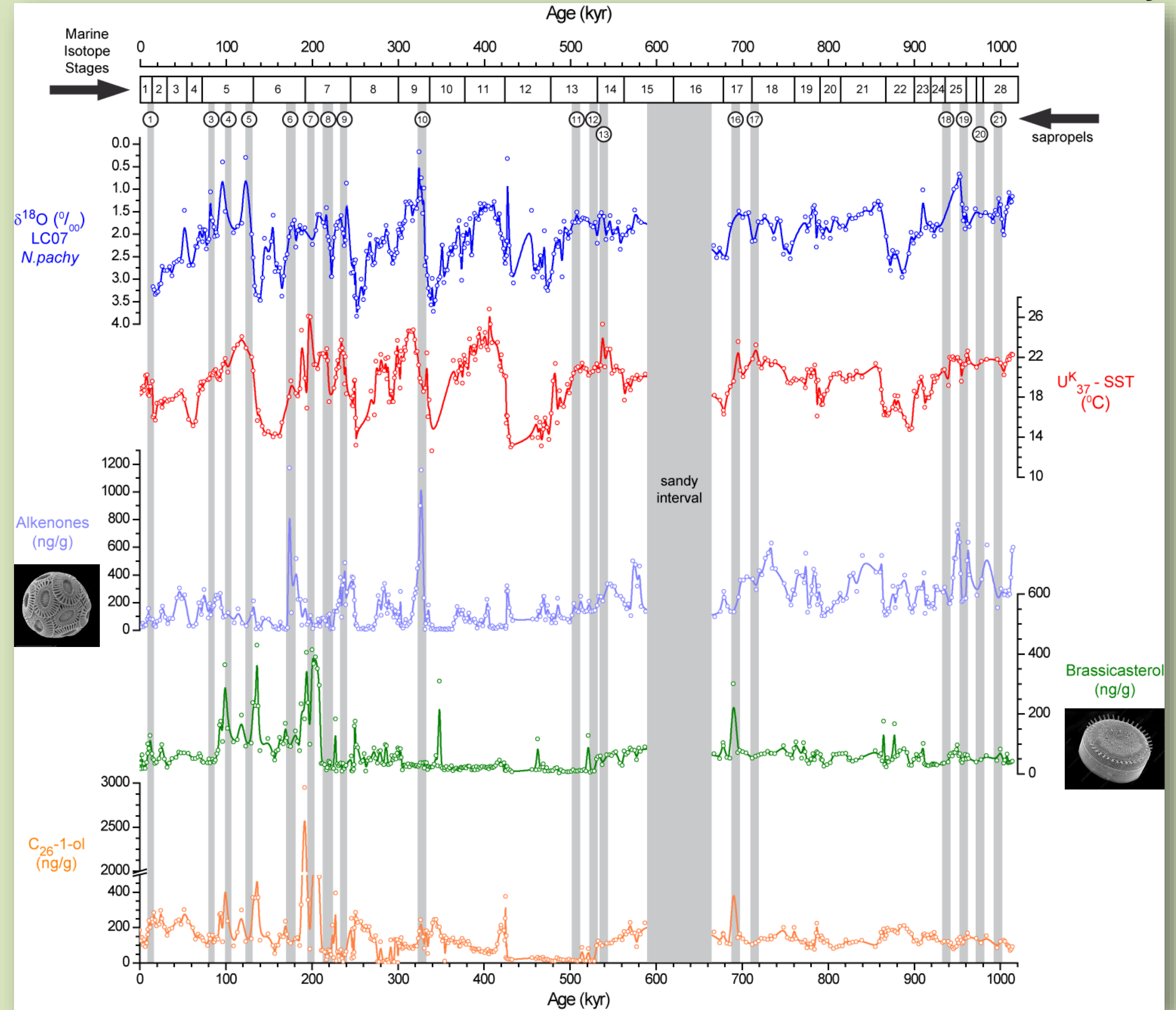


Figure 11. Molecular biomarker records from core LC07 (Martínez-Dios et al. 2021), including  $U^K_{37}$ -SSTs and the abundances of marine origin lipids (long chain alkenones, brassicasterol) together with the terrestrial n-hexacosan-1-ol concentration and the LC07 *N. pachyderma* (dextral)  $\delta^{18}\text{O}$  (data from Dinarès-Turell et al., 2003), for comparison. Grey vertical bars indicate sapropels, based on the dates from Ziegler et al. (2010) and Konijnendijk et al. (2014).

Algerian Margin

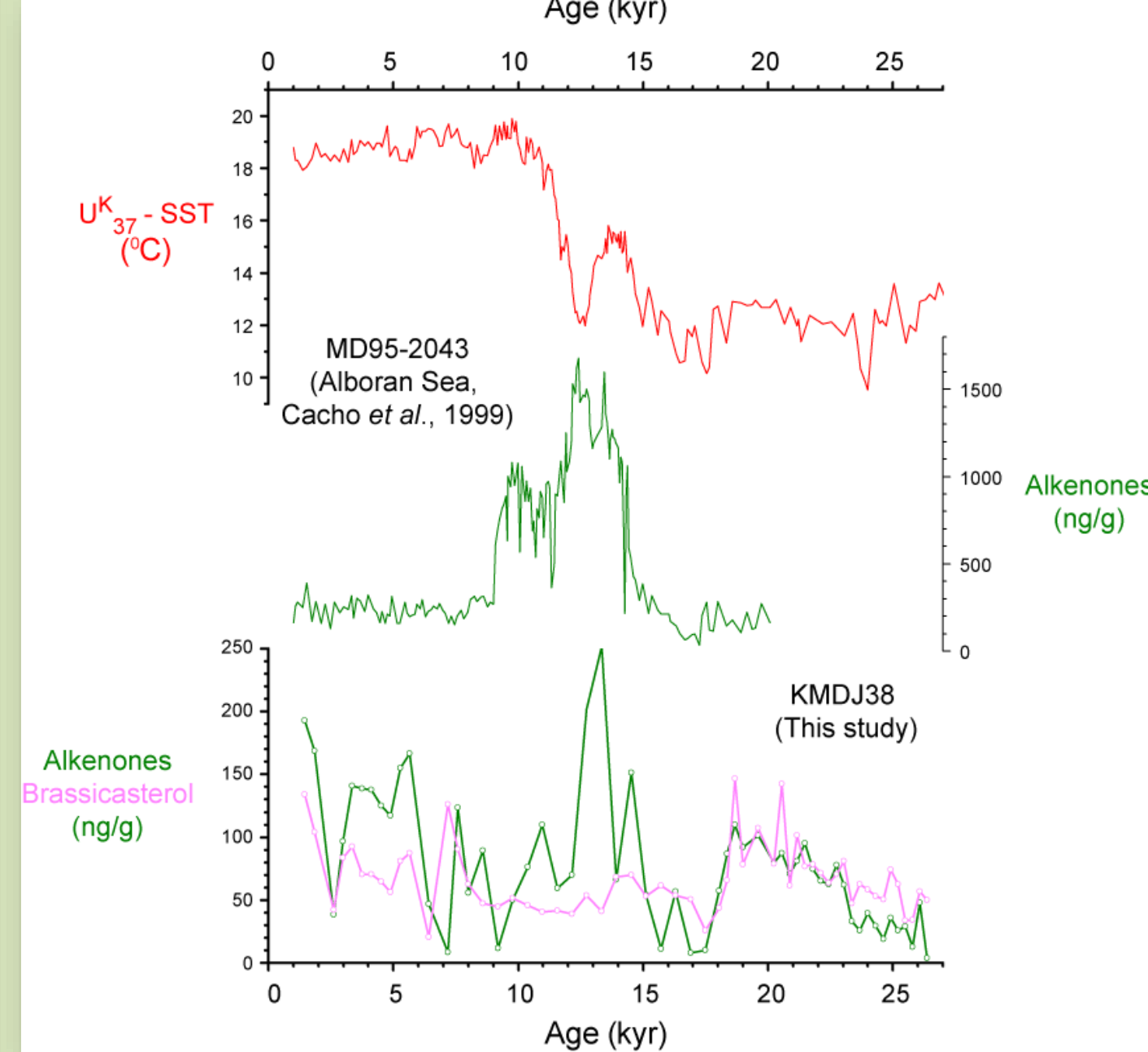


Figure 12. Abundances of phytoplankton related biomarkers from cores KMDJ38 (Algerian Margin, this study) and MD95-2043 (Alboran Sea, Cacho et al. 1999, including also the  $U^K_{37}$ -SST record from this core for reference).

## 5. Key points from this study

- A molecular biomarker record covering the last 1 million years is presented, for the first time, in the Mediterranean Sea (Figs. 7, 9, 11), together with preliminary data from the Algerian Margin (Figs. 8, 10, 12).
- SSTs in the Strait of Sicily were consistently warmer than other records located further to the west (Fig. 9) whereas, in the Algerian Margin, they resemble those in the Alboran Sea, albeit exhibiting brief warmer episodes (Fig. 10).
- In the Strait of Sicily, alternate peaks of alkenones and brassicasterol concentrations coeval to several sapropels suggest distinct proliferation of coccolithophores and diatoms during these periods (Fig. 11).
- In the Algerian Sea, a peak in the concentration of alkenones during the deglaciation, not followed by brassicasterol, matches similar results reported in the Alboran Sea, where the occurrence of an organic rich layer was described (Cacho et al. 2002).

## References:

Cacho, et al. (1999). *Paleoceanography*, 14, 698–705.  
 Cacho, et al. (2002). *Journal of Marine Systems*, 33–34, 253–272.  
 Conte et al. (2006). *G-cubed* 7, Q02005, doi:10.1029/2005GC001054.  
 Cortina et al. (2015). *Geophysical Research Letters* 42, 10,366-310,374.  
 Cortina et al. (2016). *Organic Geochemistry*, 92, 16–23.  
 Dinarès-Turell et al. (2003). *3P* 190, 195-209.  
 Giresse et al. (2013). *Sedimentary Geology*, 294, 266–281.  
 Konijnendijk et al. (2014). *Newsletters on Stratigraphy* 47, 263-282.

Lisiecki and Raymo (2005). *Paleoceanography* 20, PA1003, doi:10.1029/2004PA001071.  
 Locarnini et al., 2013. *World Ocean Atlas 2013*, Volume 1: Temperature. S. Levitus, Ed., A. Mishonov Technical Ed.; NOAA Atlas NESDIS 73, 40 pp.  
 Martínez-Dios et al. (2021) *Paleoceanogr. and Paleoclimat.* 36, doi:10.1029/2021PA004289  
 Martrat et al. (2004). *Science* 306, 1762-1765.  
 Müller et al. (1998). *Geochimica et Cosmochimica Acta*, 62, 1757–1772.  
 Powley et al. (2017). *Nutrient cycling in the Mediterranean Sea: The key to understanding how the unique marine ecosystem functions and responds to anthropogenic pressures*, in: Fuerst-Bjelliš, B. (Ed.), *Mediterranean Identities - Environment, Society, Culture*, pp. 47-77.  
 Ziegler et al. (2010). *Quaternary Science Reviews* 29, 1481-1490.

## Acknowledgements:

Financial support is acknowledged to the Spanish Ministry of Science and Innovation (SCORE and HICCUP projects) and to the Catalan Government (Research Group on Marine Biogeochemistry and Global Change). Access to core LC07 samples was kindly provided by the British Ocean Sediment Core Research Facility (BOSCORF) at the Southampton Oceanography Centre.